

Synthesis of neodymium-iron nanoperovskite for sensing applications of an antiallergic drug

Nada F. ATTA^{1,*}, Mohammad H. BINSABT², Ekram H. EL-ADS¹, Ahmed GALAL¹

¹Department of Chemistry, Faculty of Science, Cairo University, Giza, Egypt

²Department of Chemistry, Kuwait University, Safat, Kuwait

Received: 29.10.2016

Accepted/Published Online: 22.02.2017

Final Version: 05.09.2017

Abstract: A facile route was used for the fabrication of NdFeO₃ (NF) perovskite. The orthorhombic structure of single phase nanocrystalline NdFeO₃ perovskite was confirmed by different characterization techniques: XRD, FTIR, TEM, BET, SEM, and EDAX. The nanoperovskite was successfully used as a sensor component with a carbon paste electrode (CpE) for the determination of ketotifen in pharmaceutical formulations. Ketotifen, an antiallergic drug, is utilized for the treatment of asthma attacks, rhinitis, skin allergies, and anaphylaxis. Sodium dodecyl sulfate (SDS) was employed in a surface assembly mode to improve the sensitivity of the sensor response. The proposed sensor, NdFeO₃ in situ modified carbon paste electrode in the presence of SDS (NFMCPe-SDS), showed a higher current response towards ketotifen oxidation compared to other surfaces. The enhanced signal response is attributed to the catalytic properties of the sensor and the relative increase in surface area. A linear relationship between the oxidation peak current and ketotifen concentration was obtained in the concentration range of 0.8 μmol L⁻¹ to 360 μmol L⁻¹. The surface showed long-term stability of 1 month of operation and the limits of detection and quantification of ketotifen were 2.92 nmol L⁻¹ and 9.71 nmol L⁻¹, respectively, with high sensitivity of 311 μA/mmol L⁻¹. The composite electrode proved to be selective for drug sensing in the presence of different interfering species and applicable for drug determination in commercial tablets, human serum, and urine.

Key words: NdFeO₃, carbon paste electrode, ketotifen, surface active agent, real sample analysis

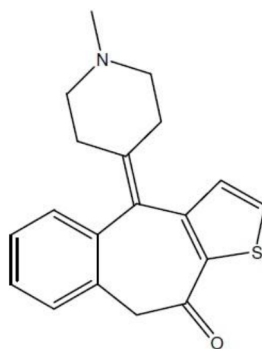
1. Introduction

Ketotifen, [4-(1-methyl-4-piperilidene)-4H-benzo-(4,5)-cyclohepta-(1,2-b)-thiophen-10(9H)-one] (Scheme), is a benzocycloheptathiophene derivative demonstrating a number of pharmacological impacts. Ketotifen, an anti-histaminic and antianaphylactic drug, is widely utilized to prohibit the development of allergic conjunctivitis, minimize the recurrence and acuteness of asthma attacks, and cure rhinitis and anaphylaxis.¹⁻⁷ Ketotifen, a selective and noncompetitive blocker of histamine H1 receptors, is used to stabilize the mast cells through the suppression of inflammatory mediators released from mast cells.^{1,4,6} In addition, it can be combined with other drugs to be used to preserve the fat-burning effects for a long time without the need for periods of on and off cycles. On the other hand, ketotifen exhibits some side effects such as sleepiness, irritability, bleeding of the nose, and drying of the mouth. It can also cause weight gain and improved insulin sensitivity within the muscle tissues as a result of increasing appetite.³ Therefore, it is a necessity to determine ketotifen selectively and sensitively.

*Correspondence: anada@sci.cu.edu.eg

Diverse analytical methods have been proposed for the selective and sensitive determination of ketotifen like atomic absorption spectrometry,⁸ spectrophotometric methods,⁹ high-performance liquid chromatography,¹⁰ and liquid chromatographic–mass spectrometric methods.¹¹ Most of these methods have some obstacles, such as low sensitivity, expensive devices, complicated processes, and being time-consuming. As a result, electrochemical methods are used as functional alternatives due to their fast response, simplicity, short analysis time, high sensitivity, and low cost. Furthermore, the electrochemical methods provide the ability of sensing the studied drug in vivo with real-time analysis and in living organisms.^{2–4} A carbon paste electrode modified with Fe₃O₄ magnetic nanoparticles coated by [3-(trimethoxysilyl)-1-propanethiol] was utilized for the electrochemical determination of ketotifen, displaying higher current response toward ketotifen oxidation compared to bare electrodes.²

Interest was expressed towards perovskite-type oxides of the general formula ABO₃ because of their fascinating catalytic activity and thermal stability. The 12-coordinated A site and the 6-coordinated B site in ABO₃ perovskite are occupied with rare earth or alkaline metals and transition metals, respectively.^{12–15} Perovskite-type oxides exhibited a wide domain of applications in various technologies like electrode materials, solid oxide fuel cells, catalysts, magnetic materials, and chemical sensors.¹² They have opened up new era for possible applications in sensors, particularly electrochemical sensors. The enormous applications of perovskites were attributed to their great electronic conductivity, oxygen content variations, oxide ion mobility within the crystal, electrically active structure, dielectric and photocatalytic properties, thermoelectric and magnetic properties, and thermal and chemical stability.¹⁵



Scheme. Structure of ketotifen.

NdFeO₃, one of the rare-earth orthoferrites, is orthorhombic distorted perovskite where FeO₆ octahedra are formed by the coordination of Fe³⁺ ions by six O²⁻ ions.^{12,16–18} The NdFeO₃ crystallographic unit cell consists of corner shared FeO₆ octahedra, resulting in the formation of a three-dimensional distorted perovskite structure. Three competing magnetic interactions in NdFeO₃, Fe–Fe, Nd–Fe, and Nd–Nd, determine its fascinating magnetic and structural properties resulting in various applications.^{16–19} NdFeO₃ was utilized as a superior catalyst for many reactions like hydrogen evolution reaction,¹³ methane combustion, and carbon dioxide oxidation.¹⁴ It was also utilized in S/O₂ solid oxide fuel cells as an anode material.²⁰ NdFeO₃ and its doped forms can provide many opportunities for improved gas sensing behavior^{21,22} like H₂S gas;¹⁶ CO gas;²³ liquefied petroleum gas;²¹ hydrocarbon gases like methane, propane, and n-hexane;²² and ethanol gas.^{16,24} Galal et al. investigated the electrocatalytic activity of NdFeO₃ prepared via microwave-assisted citrate method toward hydrogen evolution reaction. NdFeO₃ displayed superior electrocatalytic activity compared to GdFeO₃, LaFeO₃, and SmFeO₃ toward hydrogen evolution reaction in terms of low activation energy, high exchange

current density, small strength of the Fe–O bond that contains some degree of covalence, and large interionic distances (Fe–O).¹³ The electrochemical sensing application of NdFeO₃, namely for ketotifen determination, was not cited previously. Thus, this work examines the electrocatalytic activity of a NdFeO₃ (NF) modified carbon paste electrode (CpE) toward the electrochemical sensing of ketotifen drug.

Surfactants, a class of molecules with surface active properties, play important roles in electrochemistry and electroanalysis of biological compounds and drugs^{25–28} and can be used widely in the development of electrochemical sensors for drug determination.²⁹ Surfactants can be utilized as selective masking agents, improving the sensitivity and selectivity of electrochemical methods.²⁷ They can also promote the electrochemical signal of the studied analytes via various effective pathways. They have great influence on the electrode reactions via adsorption at the electrode/solution interface or aggregation in the form of supramolecule structures.^{28,29} They also can form micelles, surfactant aggregates, leading to the solubilization of organic compounds. They can supply distinctive orientation of the molecules at the surface of the electrode. In addition, they can enhance the accumulation/preconcentration of the studied analytes at the surface of the electrode.³⁰ Therefore, the redox potential, diffusion coefficients, and charge transfer coefficients of the electrode processes can be changed significantly by the surfactant adsorption and the solubilization of the studied compounds in micellar aggregates.²⁷ On the other hand, the addition of surfactant to electrolytes greatly enhances the current response, sensitivity, and selectivity by improving the electrode/solution interface properties.^{26–30} Therefore, several modified electrodes for the determination of various drugs in the presence of sodium dodecyl sulfate (SDS)^{26,27,29–31} or cetyltrimethylammonium bromide^{25,32} were proposed in literature.

This study presents for the first time a novel sensor based on the in situ modification of a carbon paste electrode with NdFeO₃ for the electrochemical determination of ketotifen in the presence of a surface active agent (NFMCPe-SDS). The orthoferrite neodymium nanocrystals were synthesized via simple microwave assisted-citrate method. Few publications mentioned the applications of NdFeO₃ in catalysis and fuel cells. In a previous study,³³ we demonstrated the formation of a “core-shell” between NdFeO₃ and ionic liquid crystals (ILCs). The core-shell composite was used successfully as a sensor for metoclopramide drug determination. The surface area and pore volume increased while pore size decreased in the case of NdFeO₃/ILCs compared to the bare perovskite. This resulted in enhanced catalytic activity evidenced by oxidation signal enhancement.³³ Thus, it is essential to evaluate the catalytic activity and sensing performance of NdFeO₃ modified CpE in the presence of a surface active agent in the absence of ILCs.

NdFeO₃ modified CpE demonstrated greater electrocatalytic activity, higher sensitivity, and better selectivity toward ketotifen in the presence of SDS compared to unmodified electrodes. The utilization of surface active agents in this work presents a novel useful dimension in ketotifen investigation using the prepared perovskite. In addition, the proposed sensor showed antiinterference ability for the determination of ketotifen in the presence of interferents.

2. Results and discussion

2.1. Characterization of NdFeO₃ perovskite

2.1.1. XRD and FTIR spectra

In the prepared NdFeO₃ perovskite, Nd³⁺ and Fe³⁺ occupied the A site and the B site, respectively. NdFeO₃ perovskite was prepared through the microwave assisted-citrate method and then sintered for 5 h at 900 °C according to our previous work.^{13,33} XRD was performed to confirm the formation of the pure single phase of

NdFeO₃ without any secondary phases³³ (Supplementary Figure 1A and Supplementary Table 1). In addition, the formation of NdFeO₃ perovskite was also confirmed by FTIR analysis (Supplementary Figure 1B).^{12,33,34} The detailed examination of the XRD and FTIR data can be found in our previous work.³³

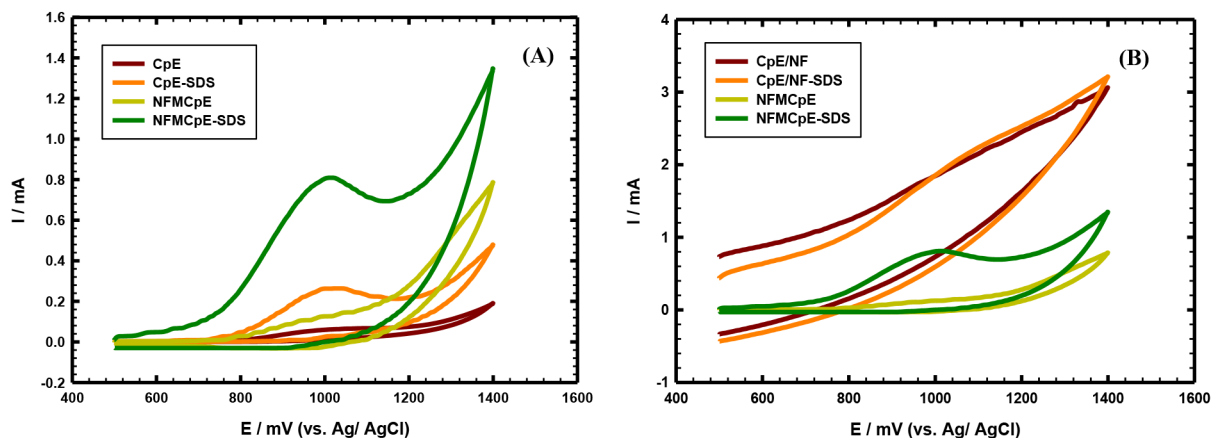


Figure 1. A) CVs of 0.5 mmol L⁻¹ ketotifen/0.1 mol L⁻¹ PBS/pH 7.40 at bare CpE, CpE-SDS, NFMCPe, and NFMCPe-SDS, scan rate 0.05 V s⁻¹. B) CVs of 0.5 mmol L⁻¹ ketotifen/0.1 mol L⁻¹ PBS/pH 7.40 at CpE/NF, CpE/NF-SDS, NFMCPe, and NFMCPe-SDS.

Table 1. EIS fitting data corresponding to Figure 3 at CpE-SDS and NFMCPe-SDS.

Electrode	m	CPE2/F cm ⁻²	C _f /F cm ⁻²	n	CPE1/F cm ⁻²	W/Ω s ^{-1/2}	R _p /Ω cm ²	C _c /F cm ⁻²	R _s /Ω cm ²
CpE-SDS	0.659	511.2	9.29 × 10 ⁻⁴	0.296	446.6	1189	3037	3.39 × 10 ⁻⁵	98.08
NFMCPe-SDS	0.977	712.9	1.25 × 10 ⁻³	0.413	3965	212.2	337.9	4.23 × 10 ⁻⁴	172.9

2.1.2. TEM, BET, and EDAX

The TEM of NdFeO₃ and its diffraction pattern are shown in Supplementary Figures 2A and 2B, respectively. The diffraction pattern of NdFeO₃ was comparable with the XRD data in Section 2.1.1. Ideal and distorted orthorhombic crystals of NdFeO₃ were observed in the TEM image with average particle size of 50 nm. High surface activity was achieved by the presence of twin and multicrystals with many edges.³³ In addition, the BET surface area of NdFeO₃ was 26.81 m²/g, indicating its great electrocatalytic activity as will be discussed in the next sections. The EDAX for NdFeO₃ confirmed the formation of NdFeO₃ perovskite (Supplementary Figure 2C).³³

2.2. Electrochemistry of ketotifen at CpE in situ modified with NdFeO₃ in the presence of SDS

The voltammetric behavior of 0.5 mmol L⁻¹ ketotifen/0.1 mol L⁻¹ PBS/pH 7.40 was examined at bare CpE and CpE in situ modified with NdFeO₃ (NFMCPe) using cyclic voltammetry as shown in Figure 1A. A broad peak at ~1.020 V with a relatively small anodic peak current was obtained in the case of bare CpE. Upon modification with 10% NdFeO₃, the anodic peak current increased slightly but the peak was broad at ~1.010 V. As mentioned in the literature,² the electrochemistry of ketotifen exhibited irreversible oxidation behavior. In the presence of 10 μL of 0.1 mol L⁻¹ SDS, the anodic peak current of 0.5 mmol L⁻¹ ketotifen/0.1 mol L⁻¹ PBS/pH 7.40 at CpE was 270 μA at the anodic peak potential of 1.018 V and the electrode was represented

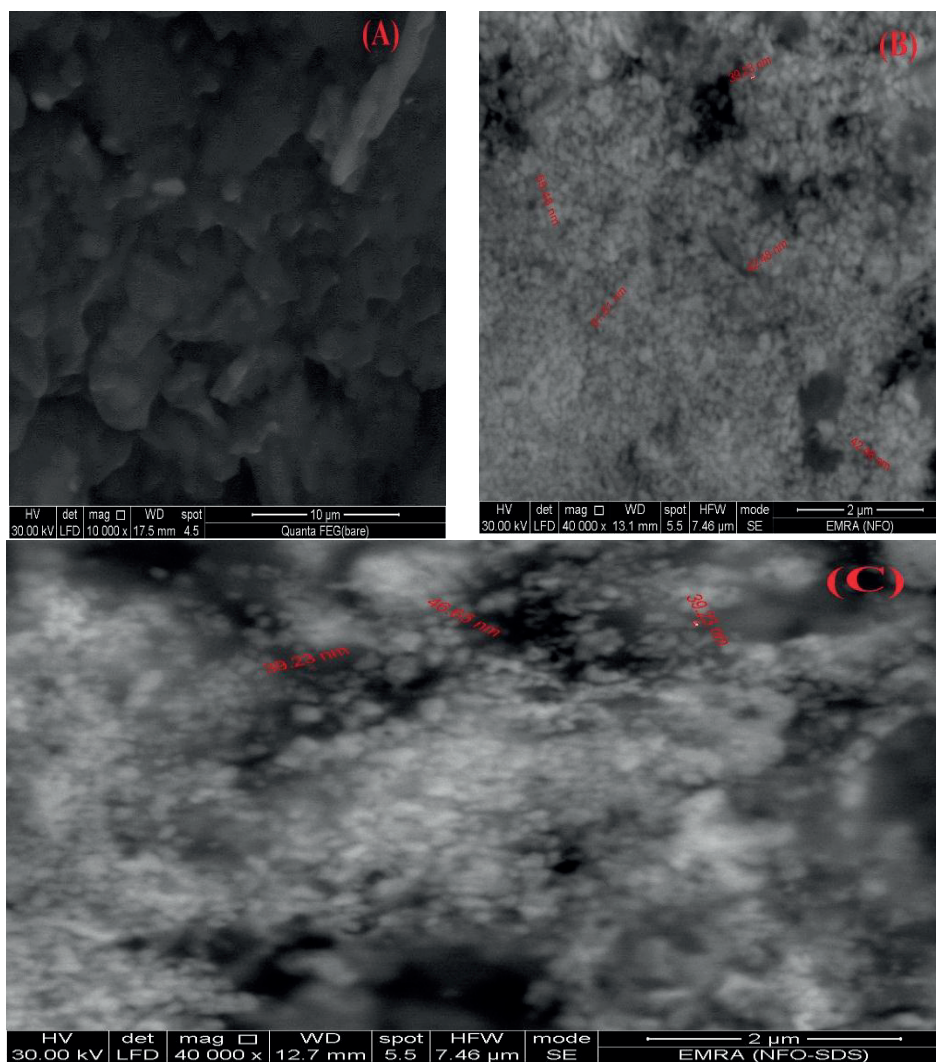


Figure 2. SEM micrographs of A) bare CpE, B) NFMCPe, and C) NFMCPe-SDS.

as CpE-SDS. At NFMCPe in the presence of 10 μL of 0.1 mol L^{-1} SDS, the anodic peak current of ketotifen increased sharply to 640 μA at the anodic peak potential of 1.011 V and the electrode was represented as NFMCPe-SDS. The voltammetric behavior at CpE, CpE-SDS, NFMCPe, and NFMCPe-SDS in 0.1 mol L^{-1} PBS/pH 7.40 showed that there are no peaks in the working potential window of ketotifen (data not shown).

At bare CpE, relatively slow electron transfer kinetics were achieved, which may be attributed to surface fouling by the oxidation product. By in situ modification with NdFeO_3 , a slight increase in the anodic peak current was obtained, which indicated a slight increase in the reaction kinetics and facilitation of electron transfer due to the catalytic properties of NdFeO_3 perovskite. The anodic peak current of ketotifen increased by 2.4-fold at NFMCPe-SDS compared to CpE-SDS, which may be attributed to the higher surface area achieved by the presence of NdFeO_3 perovskite. The presence of SDS greatly affected the anodic peak current and the sharpness of the anodic peak at CpE-SDS and NFMCPe-SDS modified electrodes. SDS facilitated the preconcentration/aggregation of ketotifen at the electrode surface, resulting in higher electron transfer kinetics. The pK_a of ketotifen is 8.43, showing that it is positively charged at the working pH (7.40).⁶ In addition,

SDS can be adsorbed on the electrode surface, forming a layer with highly dense negatively charged ends pointed outside the electrode. Therefore, there is an electrostatic interaction between the positively charged ketotifen drug and the anionic SDS that facilitates the preconcentration and aggregation of the drug at the electrode surface, therefore enhancing the current signal of ketotifen at the proposed sensor.^{26,27,29} Therefore, NdFeO₃ perovskite and SDS acted as catalytic modifiers facilitating the electron transfer rate of ketotifen at NFMCPe-SDS.

On the other hand, NdFeO₃ can be immobilized on the surface of the bare CpE from suspension containing 10 mg of NdFeO₃/1 mL of DMF, which was sonicated for 30 min and then 80 μ L of the suspension was cast on the surface and left to dry.¹⁵ This electrode was represented as CpE/NF. As observed in Figure 1B, the voltammetric behavior of ketotifen was very sluggish at CpE casted with NdFeO₃ even in the absence or presence of SDS (CpE/NF or CpE/NF-SDS, respectively). The presence of NdFeO₃ on the surface may cause blocking of the active sites of the underlying CpE and hinders the oxidation of ketotifen, even in the presence of SDS. This result suggested that the in situ modification of CpE with NdFeO₃ was more effective and suitable for the electrocatalytic oxidation of ketotifen in the presence of SDS.

The effectiveness and the catalytic performance of NFMCPe-SDS towards ketotifen oxidation can be explained in terms of surface morphology. The SEM of bare CpE (Figure 2A) showed separated layers and irregular and isolated graphite flakes. Upon modification with NdFeO₃ (Figure 2B), assemblies of NdFeO₃ nanoparticles with the average particle size of 45 nm were observed, greatly affecting the active surface area available for the reaction. Sphere-like nanostructures of NdFeO₃ were also observed with uniform morphology and particle size. In the presence of SDS (Figure 2C), spongy films of SDS were observed, which were assembled on the surface and facilitated the aggregation of ketotifen, resulting in a higher electron transfer rate.³¹

2.3. Optimization of NdFeO₃ loading in CpE

The weight % of NdFeO₃ perovskite inside the paste greatly affected the voltammetric determination of ketotifen. The relation between the oxidation peak current of 0.5 mmol L⁻¹ ketotifen/0.1 mol L⁻¹ PBS/pH 7.40 and the weight % of NdFeO₃ inside the paste was investigated (data not shown). The peak current of ketotifen increased by increasing the weight % of NdFeO₃ due to the enhanced number of active sites available for the catalytic reaction and the increased surface area. The optimal weight % of NdFeO₃ chosen was 10% as the anodic peak current is slightly the same with further increase in weight % (>10%). This may be due to higher resistance, increased noise, lower electroconductivity, and greater capacitive current.¹⁵

2.4. Effect of operational parameters

2.4.1. Effect of scan rate

The influence of different scan rates on the electrochemistry of 0.5 mmol L⁻¹ ketotifen/0.1 mol L⁻¹ PBS/pH 7.40 was investigated at CpE-SDS and NFMCPe-SDS. The inset of Supplementary Figure 3A shows the CVs of ketotifen at NFMCPe-SDS at different scan rates from 0.01 to 0.1 V s⁻¹. By increasing the scan rate, the anodic peak current increased and the anodic peak potential shifted to more positive values. The same trend was observed at CpE-SDS but with lower values of the anodic peak current (data not shown). Supplementary Figure 3A shows the linear relationship between the anodic peak current of ketotifen and the square root of the scan rate from 0.01 to 0.1 V s⁻¹ at CpE-SDS and NFMCPe-SDS. This linear relation proved that the electrocatalytic oxidation of ketotifen at CpE-SDS and NFMCPe-SDS is diffusion-controlled. The real diffusion

coefficient D_{real} of ketotifen at CpE-SDS and NFMCPe-SDS was calculated from the Randles–Sevcik equation (assuming a transfer coefficient of 0.5) using the real surface area calculated from the $[\text{Fe}(\text{CN})_6]^{4-}/[\text{Fe}(\text{CN})_6]^{3-}$ test. The electrochemistry of $5 \text{ mmol L}^{-1} [\text{Fe}(\text{CN})_6]^{4-}/[\text{Fe}(\text{CN})_6]^{3-}$ in $0.1 \text{ mol L}^{-1} \text{ KCl}$ as a supporting electrolyte at CpE-SDS and NFMCPe-SDS was explored. The active real surface area was 0.297 cm^2 in the case of CpE...SDS, which increased to 0.449 cm^2 in the case of NFMCPe-SDS. The calculated D_{real} was $1.1455 \times 10^{-4} \text{ cm}^2/\text{s}$ at CpE-SDS, which increased to $2.8077 \times 10^{-4} \text{ cm}^2/\text{s}$ at NFMCPe-SDS due to the electrocatalytic activity of this composite, resulting in facilitation of the charge transfer process at the electrode/solution interface.

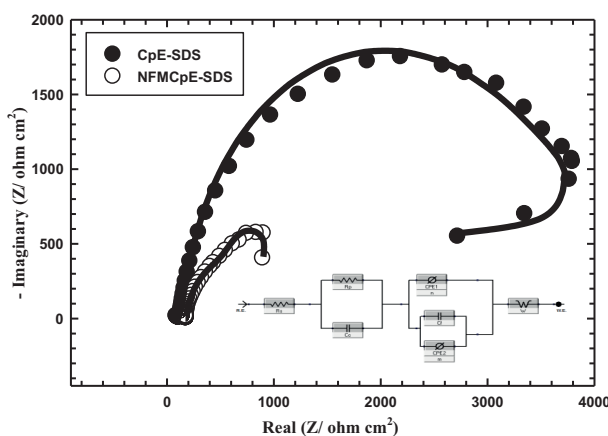


Figure 3. Nyquist plot of CpE-SDS (black circles) and NFMCPe-SDS (white circles) in 0.5 mmol L^{-1} ketotifen/ 0.1 mol L^{-1} PBS/pH 7.40 at the oxidation potential of ketotifen. Symbols and solid lines represent the experimental measurements and the computed fitting of impedance spectra, respectively; frequency range: $0.1\text{--}100,000 \text{ Hz}$. Inset: the equivalent circuit used in the fitting procedure of the impedance spectra.

On the other hand, the relation between the logarithm of the anodic peak current of ketotifen (I_{pa}/A) and the logarithm of the scan rate ($\nu/\text{mV s}^{-1}$) was linear at both CpE-SDS and NFMCPe-SDS (Supplementary Figure 3B). The linear regression equations at CpE-SDS and NFMCPe-SDS, respectively, are:

$$\text{Log}I(A) = 0.6811 \log \nu(\text{mV s}^{-1}) - 4.553,$$

and

$$\text{Log}I(A) = 0.5180 \log \nu(\text{mV s}^{-1}) - 4.039.$$

The slopes of these relations were 0.6811 and 0.5180 at CpE-SDS and NFMCPe-SDS, respectively. The first slope deviates from the theoretical value of 0.5 for diffusion-controlled processes. This result indicated that the electrocatalytic oxidation of ketotifen was controlled by diffusion rather than adsorption at the NFMCPe-SDS electrode,² while the possibility of adsorption is more likely in the case of the CpE-SDS electrode.

2.4.2. Effect of pH

The effect of the pH of the supporting electrolyte on the electrochemical response of the proposed sensor was investigated. The pH study was performed by an accumulation step at -0.2 V for 60 s and then differential pulse voltammetry (DPV) was applied. The response of the modified electrode NFMCPe-SDS was examined in 0.5 mmol L^{-1} ketotifen/ 0.1 mol L^{-1} PBS of different pH values from 2 to 11 (data not shown). From the

DPV results, the pH value of the solution displayed a great impact on the anodic peak potential and the anodic peak current of ketotifen at the surface of the modified electrode. In other words, the oxidation of ketotifen at NFMCPe-SDS is highly dependent on the pH and protonation/deprotonation steps are involved in the charge transfer process.^{2,15} In addition, as the pH shifted to higher values, the oxidation potential of ketotifen shifted to less positive values (Supplementary Figure 4). This is attributed to the deprotonation that was involved in the oxidation process and facilitated at high pH. The relation between the oxidation potential of ketotifen and pH can be expressed using the following linear regression equation:

$$E_{pa}(V) = 1.35 - 0.051pH.$$

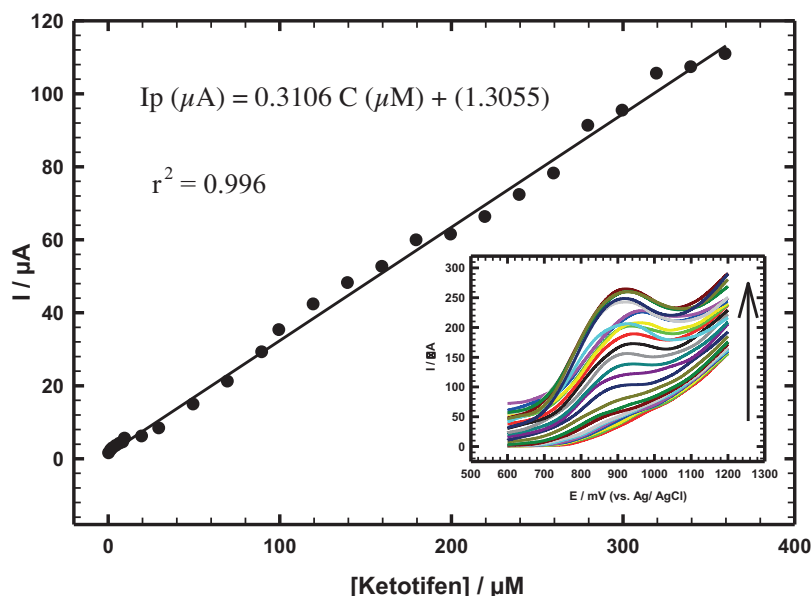
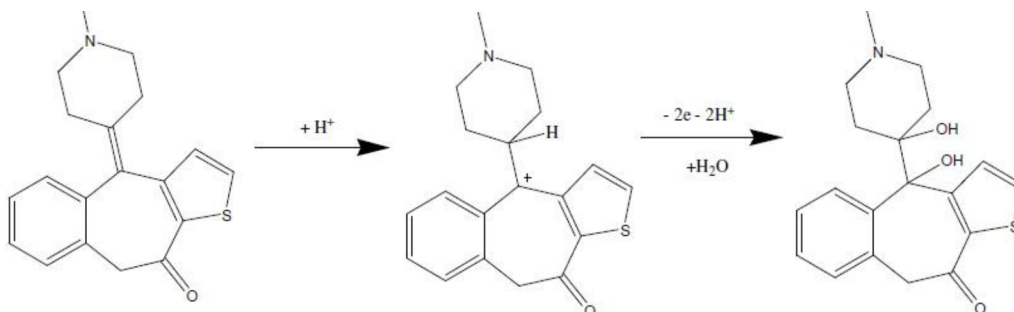


Figure 4. Calibration curve for ketotifen for concentrations from $0.8 \mu\text{mol L}^{-1}$ to $360 \mu\text{mol L}^{-1}$. Inset: DPV of 15 mL of 0.1 mol L^{-1} PBS/pH 7.40 at NFMCPe-SDS in different concentrations of ketotifen ($0.8 \mu\text{mol L}^{-1}$ to $360 \mu\text{mol L}^{-1}$).

The correlation coefficient is 0.991 (over the pH range 2–11). The slope (-0.051 V/pH) is close to the Nernstian slope (-0.059 V/pH), indicating that the oxidation reaction of ketotifen was achieved by two-electron/two-proton transfer. The oxidation reaction of ketotifen can be described as follows:²



Moreover, the oxidation peak current of ketotifen was highly influenced by the pH value, as indicated in the inset of Supplementary Figure 4. Upon increasing the pH, the oxidation peak current increased, reaching

its maximum value at pH 8, and then decreased again. The pH of the study was 7.4 (the physiological pH of the human body).

2.5. Electrochemical impedance spectroscopy (EIS)

The electrode surface/electrolyte interface plays a crucial role in the electron transfer process. Thus, EIS measurements are used for the electronic properties at the interface.¹⁵ EIS was carried out in a solution containing 0.5 mmol L⁻¹ ketotifen/0.1 mol L⁻¹ PBS/pH 7.40 at the oxidation potentials over an AC frequency ranging from 0.1 to 100 kHz for CpE-SDS and NFMCPe-SDS modified electrodes. Figure 3 shows the EIS spectra in the form of Nyquist plots at CpE-SDS and NFMCPe-SDS modified electrodes. The equivalent circuit (the inset of Figure 3) used in fitting the experimental results contained the solution resistance (R_s), the polarization resistance (R_p), the Warburg impedance due to diffusion (W), and the double layer and film capacitances (C_c and C_f). In addition, $CPE1$ and $CPE2$ are used, resembling the predominant diffusion influence on the charge transfer process with their corresponding exponents (n and m). CPE can be used as a substitute for a pure capacitor or resistor in order to compensate for nonideal conditions at the interface reflecting the inhomogeneity and defects on the surface.

The best fitting values calculated from the equivalent circuit for the impedance data are summarized in Table 1. An obvious decrease in the values of R_p and W was observed upon modifying the CpE-SDS with NdFeO₃ (NFMCPe-SDS), reflecting less electronic resistance, higher conductivity, enhanced diffusion, and more facilitation of the charge transfer. This is due to the high conductivity and catalytic activity of NdFeO₃. In addition, there is an increase in the values of capacitances C_c and C_f upon modification, reflecting the conducting character of the proposed sensor as a result of the charge transfer process. In addition, there is an obvious increase in the values of $CPE1$ and $CPE2$, which resemble pure capacitors in our case, reflecting the conducting nature of the modified surface. The previous results indicated that both NdFeO₃ and SDS play very important roles in the decrease of the charge transfer resistance and the enhancement of the electron transfer rate at the electrode/solution interface.

2.6. Method validation

Method validation was achieved through a series of experiments such as linearity, detection limit, quantification limit, accuracy, precision, specificity, selectivity, and robustness under the optimized parameters. The electrochemical determination of ketotifen was investigated at NFMCPe-SDS using DPV. Figure 4 (the inset) shows the DPV of standard additions of 1 mmol L⁻¹ ketotifen/0.1 mol L⁻¹ PBS/pH 7.40 to 15 mL of 0.1 mol L⁻¹ PBS/pH 7.40. There is a linear relation between the anodic peak current and the concentration of ketotifen in the concentration range of 0.8 μ mol L⁻¹ to 360 μ mol L⁻¹. The calibration curve of the anodic peak current of ketotifen in this linear range is shown in Figure 4. The regression equation of this calibration curve was:

$$I_p(\mu A) = 0.3106C(\mu mol L^{-1}) + (1.3055).$$

The following are the figures of merit: correlation coefficient (r^2) = 0.996, sensitivity = 310.6 μ A/mmol L⁻¹, detection limit = 2.92 nmol L⁻¹, and quantification limit = 9.71 nmol L⁻¹. Table 2 contains a comparison for determination of ketotifen based on literature reports showing lower detection limit, wider linear dynamic range, and higher sensitivity compared to other electrodes and techniques.^{2-4,35-38} Therefore, the proposed sensor showed good sensing performance toward ketotifen oxidation in terms of limit of detection and sensitivity.

Table 2. Comparison for determination of ketotifen at various modified electrodes based on literature reports.

Electrode	Technique	Electrolyte	LDR (mmol L ⁻¹)	Sensitivity (μA mmol ⁻¹ L cm ⁻²)	LOD (μmol L ⁻¹)
Carbon paste electrode modified by magnetic core-shell Fe ₃ O ₄ [2]	Voltammetric	Britton-Robinson buffer solution (pH 7)	5 × 10 ⁻⁷ to 3.0 × 10 ⁻⁵ mol L ⁻¹	186.6 μA/mmol L ⁻¹	45 nmol L ⁻¹
PVC membrane electrode [3]	Flow injection analysis	Not reported	1.0 × 10 ⁻⁵ to 1.0 × 10 ⁻² mol L ⁻¹	Not reported	4.60
Carbon paste electrode [4]	Potentiometric	Not reported	10 ⁻⁷ to 10 ⁻² mol L ⁻¹	Not reported	98.1 nmol L ⁻¹
Coated graphite membrane [35]	Potentiometric	Not reported	5.0 × 10 ⁻⁶ to 1.0 × 10 ⁻² mol L ⁻¹	Not reported	5.0
Hanging mercury drop electrode [36]	Adsorptive stripping voltammetric	Britton-Robinson buffer solution (pH 11)	5 × 10 ⁻⁸ to 1 × 10 ⁻⁶ mol L ⁻¹	Not reported	0.7 nmol L ⁻¹
Tris(1,10 phenanthroline) ruthenium(II)-Ce(IV) system [37]	Chemiluminescence	Not reported	8 × 10 ⁻⁷ to 8 × 10 ⁻⁵ mol L ⁻¹	Not reported	0.2
Ion-pair with bromothymol blue [38]	Spectrophotometric	Not reported	7 × 10 ⁻⁷ to 6 × 10 ⁻⁵ mol L ⁻¹	Not reported	0.5
NFMCpE-SDS (this work)	Voltammetric	0.1 M PBS/pH 7.4	0.8 μmol L ⁻¹ to 360 μmol L ⁻¹	310.6 μA/mmol L ⁻¹	2.92 nmol L ⁻¹

On the other hand, the robustness of the suggested method was estimated by the stability of the peak current under the effect of proposed minor changes in the experimental conditions. The studied variables included pH change (7.4 ± 0.2), the time before measurement ($2 \text{ min} \pm 2 \text{ s}$), and NdFeO₃ content ($10 \pm 0.1\% \text{ W/W}$). The relative standard deviations were 0.68%, 0.89%, and 0.92%, respectively. In addition, 10 measurements were carried out using one modified electrode with relative standard deviation of 0.99%. The previous results indicated that these minor changes in the experimental conditions had no impact on the current response of the proposed sensor toward the studied drug. Thus, the suggested method was reliable during normal operation.

Moreover, the intraday precision was estimated by the analysis of the same concentration in a single assay run three times with RSD of 0.87%. Interday precision was estimated by the analysis of the same concentration in three separate assay runs three times with RSD of 1.00%. These results demonstrated that good reproducibility, excellent precision, and stable response were obtained at the modified electrode. The proposed method was suitable for the quality control analysis of ketotifen based on the good precision obtained by the modified electrode.

2.7. Analytical applications

The proposed sensor was evaluated for the determination of ketotifen in real samples of human urine and blood serum and pharmaceutical formulations. These analyses were undertaken to examine the applicability of the proposed method for analysis. A linear calibration curve of ketotifen in diluted urine was obtained in the linear range of $0.8 \mu\text{mol L}^{-1}$ to $340 \mu\text{mol L}^{-1}$ (data not shown) with detection limit of 2.90 nmol L^{-1} , quantification limit of 9.62 nmol L^{-1} , and correlation coefficient of 0.995. In the case of blood serum, the linear calibration

curve of ketotifen in diluted blood serum was obtained in the linear range of $1 \mu\text{mol L}^{-1}$ to $280 \mu\text{mol L}^{-1}$ (data not shown) with detection limit of 4.06 nmol L^{-1} , quantification limit of $13.54 \text{ nmol L}^{-1}$, and correlation coefficient of 0.993.

The accuracy and precision of the proposed method in urine analysis were evaluated by choosing five different concentrations and repeating them five times (Table 3). Acceptable recovery results were obtained in the range of 97.1% to 101.3%, indicating that this method was free from interferences of the urine matrix. The relative standard deviation was in the range of 0.15% to 1.71%, indicating excellent reproducibility of the proposed method. In conclusion, ketotifen can be determined sensitively and selectively in urine samples and blood serum with a very low detection limit and high sensitivity.

Table 3. Evaluation of the accuracy and precision of the proposed method for the determination of ketotifen in urine samples.

$\text{SE}^d \times 10^{-7}$	RSD ^c (%)	$\text{SD}^b \times 10^{-7}$	Recovery (%)	Concentration of found ketotifen ($\mu\text{mol L}^{-1}$) ^a	Concentration of ketotifen added ($\mu\text{mol L}^{-1}$)
0.61	1.71	0.863	101.3	5.06	5
5.68	1.66	8.04	97.1	48.5	50
5.68	0.57	8.04	100.9	141.3	140
3.68	0.26	5.20	99.5	198.9	200
3.33	0.15	4.71	99.7	318.9	320

^aAverage of five determinations.

^bStandard deviation.

^cRelative standard deviation.

^dStandard error = $\text{SD}/n^{1/2}$.

On the other hand, the specificity of the suggested method was estimated by measuring its ability to detect ketotifen in its pharmaceutical formulation without interference from the excipients that are usually present. The determination of ketotifen in its commercial tablets (tablets of Allerban S.R., containing 2 mg ketotifen/tablet) was achieved to prove the validity of the proposed method. Standard ketotifen from the national organization for drug control and research was injected into the electrolytic cell (with concentration of $2 \mu\text{mol L}^{-1}$). Standard additions of ketotifen tablets were injected with concentrations of $5 \mu\text{mol L}^{-1}$ to $200 \mu\text{mol L}^{-1}$ (Table 4). The concentration of the analyzed sample was calculated from the following equation:

$$[\text{Standard added } (2\mu\text{mol L}^{-1}) + \text{tablet added } (5 - 200\mu\text{mol L}^{-1})].$$

Good matching between the obtained data and the expected concentrations was obtained. Table 4 shows that the proposed method was valid for determination of ketotifen in its commercial tablets without any interference from the pharmaceutical ingredients of the drug. Good recovery results were obtained in the range of 97.9% to 101.5% and the relative standard deviation was in the range of 0.18% to 2.16%. The previous results proved the ability of the proposed sensor for the sensitive and selective determination of ketotifen in its commercial tablets with good reproducibility and accuracy. The obtained recovery and relative standard deviation values were compared with those obtained using a previously reported method (direct potentiometric determination of ketotifen at carbon paste electrode).⁴ The recovery results of the reported method were in the range of 97.97% to 98.96% and the relative standard deviation was in the range of 0.74% to 1.73%. The obtained results were comparable with those obtained using the reported potentiometric method, confirming the validity of the proposed method for quality control assessment of ketotifen.⁴

Table 4. Recovery data obtained by standard addition method for ketotifen in drug formulation.

SE ^d × 10 ⁻⁷	RSD ^c (%)	SD ^b × 10 ⁻⁷	Recovery (%)	Found (μmol L ⁻¹) ^a	Standard added (μmol L ⁻¹)	Tablet taken (μmol L ⁻¹)
1.06	2.16	1.49	97.9	6.90	2.00	5
1.14	0.23	1.61	98.8	71.2	2.00	70
1.56	0.18	2.20	101.3	123.5	2.00	120
2.79	0.22	3.94	99.3	180.7	2.00	180
4.90	0.34	6.93	101.5	205	2.00	200

^aAverage of five determinations.^bStandard deviation.^cRelative standard deviation.^dStandard error = SD/ n^{1/2}.

2.8. Interference study

It is necessary to examine the ability of the proposed sensor to selectively and simultaneously discriminate between the studied drug and the interfering species present in human fluids. Dopamine (DA) and epinephrine (EP) are very important catecholamine neurotransmitters that may interfere with the studied drug. Morphine (MO) is one of the narcotic drugs that can interfere with the drug if the patient takes it. Acetaminophen (APAP) or paracetamol is a pain-relief drug. Therefore, it is very important to investigate the ability of the proposed sensor to distinguish between the studied drug and these other interferents. In addition, ascorbic acid (AA) and uric acid (UA) are present in biological fluids and considered some of the most common interferents.¹⁵ Figures 5A–5D show the DPV results of equimolar mixtures of 0.5 mmol L⁻¹ of ketotifen and each of DA, EP, APAP, and MO at CpE-SDS and NFMCPe-SDS, respectively. Figure 5E shows the DPV of a mixture of 0.5 mmol L⁻¹ ketotifen, 5 mmol L⁻¹ AA, and 5 mmol L⁻¹ UA at CpE-SDS and NFMCPe-SDS. Unresolved combined peaks with small anodic peak current were obtained at CpE-SDS in all cases while resolved well-separated anodic peaks with higher current response and good peak potential separation were obtained at NFMCPe-SDS for all the studied cases. Glucose is also present in the biological fluid, with concentrations ranging between 4 and 6 mmol L⁻¹, and it is very important to investigate the response of NFMCPe-SDS toward ketotifen oxidation in the presence of glucose.³⁹ The DPV of 0.5 mmol L⁻¹ ketotifen at NFMCPe-SDS in the absence and presence of 5 mmol L⁻¹ glucose proved that the presence of glucose does not affect the response of the proposed sensor toward ketotifen (data not shown). The previous results showed that the proposed sensor can effectively detect ketotifen even in presence of common interferents, pain relief drugs, neurotransmitters, or narcotics. The simultaneous determination of ketotifen and other interferents can be achieved well at the surface of the proposed sensor.

2.9. Stability and reproducibility of the proposed sensor

One of the factors affecting the performance of the proposed sensor is the repeated cycle stability. Figure 6 (the inset) shows the repeated cycle stability of NFMCPe-SDS in 0.5 mmol L⁻¹ ketotifen/0.1 mol L⁻¹ PBS/pH 7.40 up to 30 cycles. Very stable response was obtained without any decrease in the anodic peak current, demonstrating that the proposed sensor was free from fouling by the oxidation products. In addition, the interelectrode precision was estimated by using four similarly prepared modified electrodes of NFMCPe-SDS independently for determination of ketotifen. Very low relative standard deviation of 0.73% was obtained. This result confirmed the advantages of the modified electrode like good reproducibility, excellent precision, and stable response.

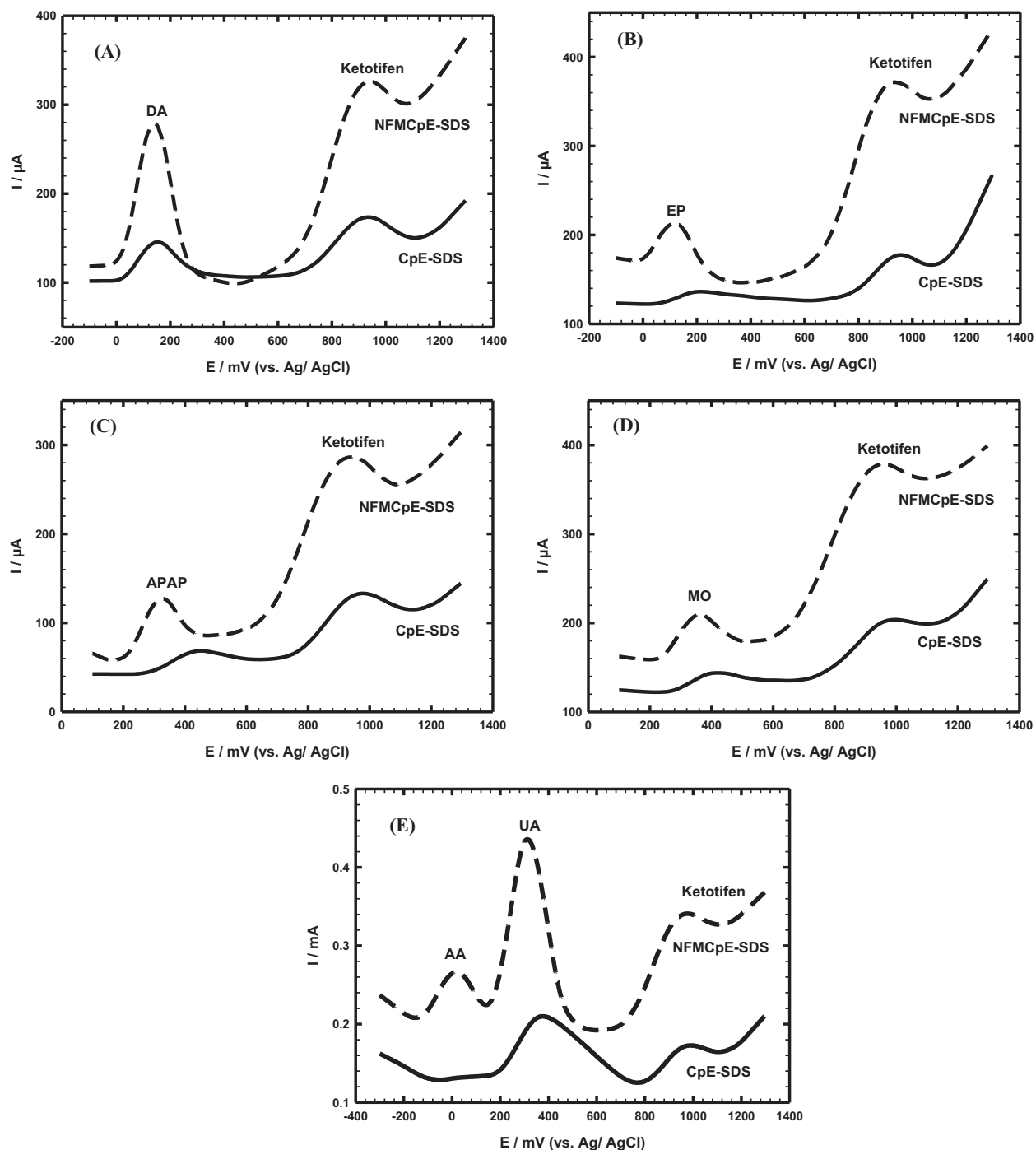


Figure 5. DPV of mixtures of A) 0.5 mmol L^{-1} DA and 0.5 mmol L^{-1} ketotifen, B) 0.5 mmol L^{-1} EP and 0.5 mmol L^{-1} ketotifen, C) 0.5 mmol L^{-1} APAP and 0.5 mmol L^{-1} ketotifen, D) 0.5 mmol L^{-1} MO and 0.5 mmol L^{-1} ketotifen, and E) 0.5 mmol L^{-1} ketotifen, 5 mmol L^{-1} AA, and 5 mmol L^{-1} UA prepared in 0.1 mol L^{-1} PBS/pH 7.40 at CpE-SDS (solid line) and NFMCPe-SDS (dashed line).

Moreover, Figure 6 shows the long-term stability of NFMCPe-SDS in 0.5 mmol L^{-1} ketotifen/ 0.1 mol L^{-1} PBS/pH 7.40 for up to 1 month of storage. The proposed sensor exhibited excellent operational stability

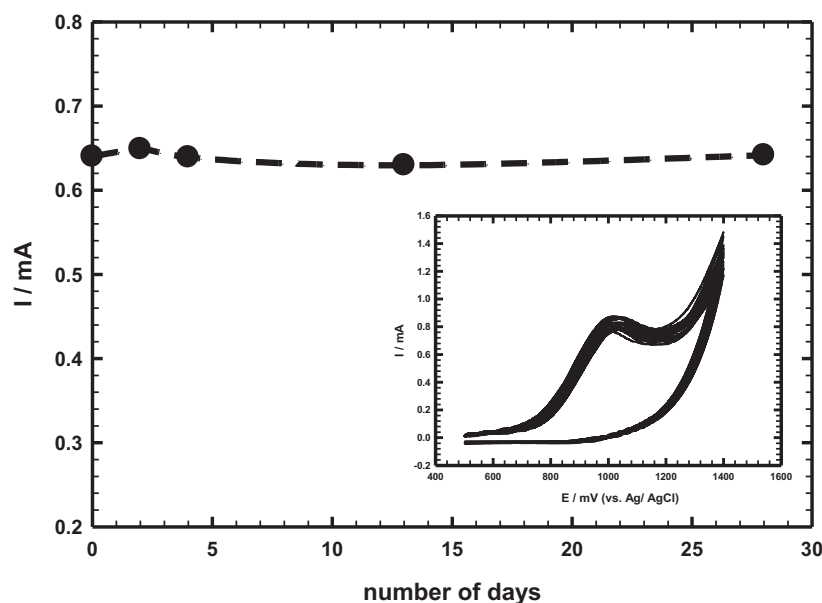


Figure 6. Variation of ketotifen oxidation peak current at NFMCPe-SDS in 0.5 mmol L^{-1} ketotifen/ 0.1 mol L^{-1} PBS/pH 7.40 taken over a period of 1 month. Inset: CVs of repeated cyclic stability of NFMCPe-SDS in 0.5 mmol L^{-1} ketotifen/ 0.1 mol L^{-1} PBS/pH 7.40, 30 repeated cycles, scan rate 0.05 V s^{-1} .

for up to 1 month of storage without any change in its response, reflecting the long lifetime of the proposed sensor.

In conclusion, a carbon paste electrode in situ modified with NdFeO_3 was presented for the first time for the voltammetric determination of ketotifen in the presence of a surface active agent. Nanocrystalline single phase NdFeO_3 oxides with an orthorhombic structure were prepared by microwave assisted-citrate method and structure confirmation was achieved by XRD, TEM, FTIR, EDAX, and SEM. NFMCPe-SDS exhibited greater electrocatalytic activity toward ketotifen determination compared to other electrodes. This is attributed to the catalytic activity of the nanocrystalline NdFeO_3 and the impact of SDS to enhance the accumulation/preconcentration of ketotifen at the electrode/solution interface, resulting in higher charge transfer rate. Also, the greater electrocatalytic activity of the proposed sensor was related to the higher real active surface area offered by NdFeO_3 nanoperovskite. A very low detection limit of 2.90 nmol L^{-1} and 4.06 nmol L^{-1} was achieved in urine samples and blood serum, respectively. The simultaneous determination of ketotifen and common interferences, pain relief drugs, neurotransmitters, or narcotics can be achieved well at the surface of the proposed sensor. The proposed sensor has good performance in terms of selectivity, wide linearity range, sensitivity, low detection limit, applicability in real samples (urine, blood, and pharmaceutical tablets), long-term stability, and antiinterference ability.

3. Experimental

3.1. Chemicals and reagents

All chemicals were used as received without further purification. Neodymium nitrate hexahydrate, ferric nitrate, citric acid, SDS, nitric acid, and ammonium hydroxide were received from Sigma-Aldrich. Graphite powder (Sigma-Aldrich, $< 20 \mu\text{m}$, synthetic) and paraffin oil (Fluka) were used to prepare the carbon paste electrode. Ketotifen was received from the national organization for drug control and research, Giza, Egypt. EP, DA, UA,

AA, APAP, MO, glucose, potassium ferrocyanide, and potassium ferricyanide were supplied by Aldrich Chem. Co. Aqueous solutions were prepared using deionized water. The supporting electrolyte was PBS ($1 \text{ mol L}^{-1} \text{ K}_2\text{HPO}_4$ and $1 \text{ mol L}^{-1} \text{ KH}_2\text{PO}_4$) of pH 2–11 and $0.1 \text{ mol L}^{-1} \text{ H}_3\text{PO}_4$ and $0.1 \text{ mol L}^{-1} \text{ KOH}$ were used to adjust the pH.

3.2. Preparation of NdFeO_3 perovskite

NdFeO_3 was prepared by the microwave assisted-citrate method as previously reported.^{13,33}

3.3. Electrochemical cells and equipment

A standard three-electrode/one-compartment glass cell was used to carry out the electrochemical characterization. A carbon paste electrode (CpE, diameter: 6.3 mm), a platinum electrode with large surface area, and a Ag/AgCl (4 M KCl saturated with AgCl) electrode were the working electrode, the auxiliary electrode, and the reference electrode, respectively. A BAS-100B electrochemical analyzer (Bioanalytical Systems) was used to perform the electrochemical characterization. The EIS was performed using a Gamry-750 instrument. SEM, EDAX, TEM, XRD, FTIR, and BET were performed using the instruments mentioned in our previous work.³³

3.4. Electrode preparation

Bare CpE was prepared by mixing graphite powder (1 g) with paraffin oil (600 μL) in a glassy mortar.³³ CpE modified with NdFeO_3 perovskite was prepared by mixing different ratios of graphite powder with NdFeO_3 to keep the total percent of the modified graphite at 100% and then mixed with paraffin oil (250 μL) to obtain a homogeneous paste. NdFeO_3 modified CpE was represented as NFMCPe. The electrochemistry of 0.5 mmol L^{-1} ketotifen/ 0.1 mol L^{-1} PBS/pH 7.4 was investigated at CpE and NFMCPe in the presence of 10 μL of 0.1 mol L^{-1} SDS. The resulting electrodes are represented as CpE-SDS and NFMCPe-SDS, respectively.³³

Another method was used for the modification of CpE with NdFeO_3 , the immobilization method. For this, 10 mg of NdFeO_3 was added to 1 mL of DMF and then sonicated for 30 min. Then 80 μL of the suspension was cast on the surface and left to dry.¹⁵ This electrode was represented as CpE/NF.

3.5. Real sample analysis

The direct analysis of the studied compound in human urine samples or blood serum was used to confirm the application of the proposed method in real sample analysis. The urine sample or blood serum used was diluted 400 times with 0.1 mol L^{-1} PBS/pH 7.4 in order to reduce the real sample's matrix effect.¹⁵ Ketotifen stock solution (1 mmol L^{-1}) was prepared in 0.1 mol L^{-1} PBS/pH 7.40 and then standard additions were carried out from the stock solution in 15 mL of diluted urine or blood serum.

3.6. Application on tablets

Determination of ketotifen in its pharmaceutical formulation was performed simply without any extraction steps or sample pretreatment. Two tablets of Allerban S.R. containing ketotifen (2 mg ketotifen/tablet) were weighed and the average mass per tablet was determined. After grinding these tablets into a fine powder, the fine powder was dissolved in 0.1 M PBS/pH 7.40 to prepare a stock solution of ketotifen (0.5 mmol L^{-1}).

Acknowledgment

The financial support from Cairo University through the Vice President's Office for Research Funds is acknowledged.

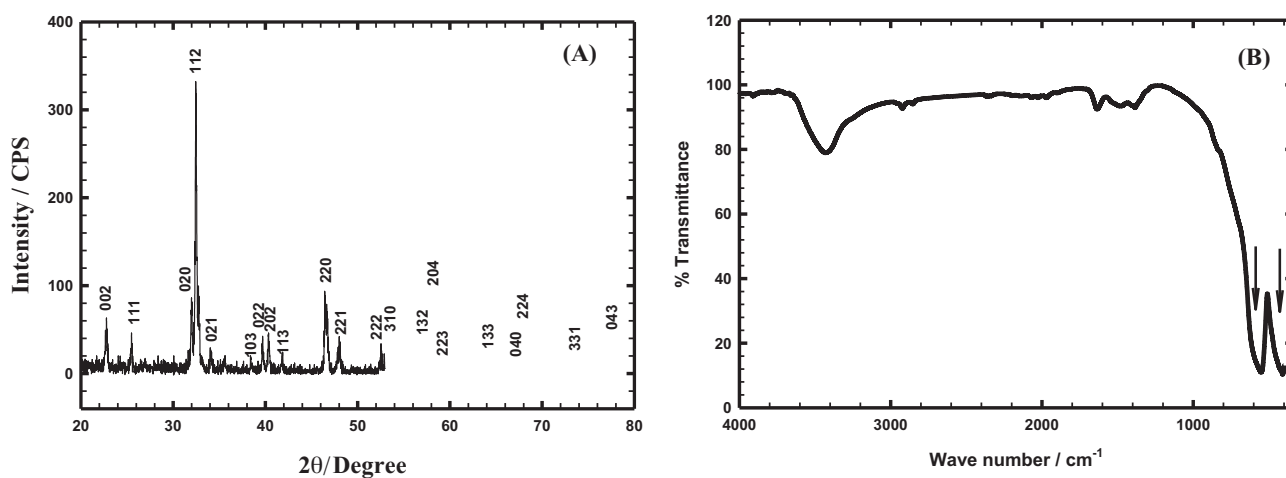
References

1. Tabrizvand, G.; Sabzi, R. E.; Farhadi, K. *J. Solid State Electrochem.* **2007**, *11*, 103-108.
2. Mashhadizadeh, M. H.; Jeilanpour, H. *Anal. Bioanal. Chem.* **2014**, *6*, 308-320.
3. Khater, M. M.; Issa, Y. M.; Mohammed, S. H. *Bioelectrochemistry* **2009**, *77*, 53-59.
4. Frag, E. Y. Z.; Mohamed, G. G.; Khalil, M. M.; Hwehy M. M. A. *Int. J. Anal. Chem.* **2011**, *2011*, 604741.
5. http://www.medicinenet.com/ketotifen-oral_tablet/article.htm.
6. <http://www.drugbank.ca/drugs/DB00920>.
7. <https://en.wikipedia.org/wiki/Ketotifen>.
8. El-Kousy, N.; Bebawy, L. I. *J. Pharm. Biomed. Anal.* **1999**, *20*, 671-679.
9. Singhvi, I.; Sachdeva, D. *Indian J. Pharm. Sci.* **2009**, *71*, 66-68.
10. Nnane, I. P.; Damani, L. A.; Hutt, A. *J. Chromatographia* **1998**, *48*, 797-802.
11. Alali, F. Q.; Tashtoush, B. M.; Najib, N. M. *J. Pharm. Biomed. Anal.* **2004**, *34*, 87-94.
12. Khorasani-Motlagh, M.; Noroozifar, M.; Yousefi, M.; Jahani, S. *Int. J. Nanosci. Nanotechnol.* **2013**, *9*, 7-14.
13. Atta, N. F.; Galal, A.; Ali, S. M. *Int. J. Electrochem. Sci.* **2014**, *9*, 2132-2148.
14. Ciambelli, P.; Cimino, S.; De Rossi, S.; Lisi, L.; Minelli, G.; Porta, P.; Russo, G. *Appl. Catal. B.* **2001**, *29*, 239-250.
15. Atta, N. F.; Ali, S. M.; El-Ads, E. H.; Galal, A. *Electrochim. Acta* **2014**, *128*, 16-24.
16. Sławiński, W.; Przeniosło, R.; Sosnowska, I.; Brunelli, M.; Bieringer, M. *Nucl. Instrum. Methods Phys. Res. B.* **2007**, *254*, 149-152.
17. Tiwari, A. *J. Alloys Compd.* **1998**, *274*, 42-46.
18. Chanda, S.; Saha, S.; Dutta, A.; Sinha, T. P. *Mater. Res. Bull.* **2013**, *48*, 1688-1693.
19. Parida, S. C.; Dash, S.; Singh, Z.; Prasad, R.; Jacob, K. T.; Venugopal, V. *J. Solid State Chem.* **2002**, *164*, 34-41.
20. Tongyun, C.; Liming, S.; Feng, L.; Weichang, Z.; Qianfeng, Z.; Xiangfeng, C. *J. Rare Earths* **2012**, *30*, 1138-1141.
21. Singh, S.; Singh, A.; Yadav, B. C.; Dwivedi, P. K. *Sens. Actuators B* **2013**, *177*, 730-739.
22. Giang, H. T.; Duy, H. T.; Ngan, P. Q.; Thai, G. H.; Thu, D. T. A.; Thu, D. T.; Toan, N. N. *Sens. Actuators B* **2011**, *158*, 246-251.
23. Ru, Z.; Jifan, H.; Zhouxiang, H.; Ma, Z.; Zhanlei, W.; Yongjia, Z.; Hongwei, Q. *J. Rare Earths* **2010**, *28*, 591-595.
24. Liu, X.; Hu, J.; Cheng, B.; Qin, H.; Jiang, M. *Curr. Appl. Phys.* **2009**, *9*, 613-617.
25. Shankar, S. S.; Swamy, B. E. K. *Int. J. Electrochem. Sci.* **2014**, *9*, 1321-1339.
26. Shrivastav, R.; Satsangee, S. P.; Jain, R. *ECS Trans.* **2013**, *50*, 23-36.
27. Bozal-Palabiyik, B.; Kurbanoglu, S.; Gumustas, M.; Uslu, B.; Ozkan, S. A. *Rev. Roum. Chim.* **2013**, *58*, 647-658.
28. Gupta, V. K.; Jain, R.; Radhapyari, K.; Jadon, N.; Agarwal, S. *Anal. Biochem.* **2011**, *408*, 179-196.
29. Teradal, N. L.; Kalanur, S. S.; Prashanth, S. N.; Seetharamappa, J. *J. Appl. Electrochem.* **2012**, *42*, 917-923.
30. Jain, R.; Sharma, S. *J. Pharm. Anal.* **2012**, *2*, 56-61.
31. Atta, N. F.; Galal, A.; El-Ads, E. H. *Electrochim. Acta* **2012**, *69*, 102-111.
32. Brahman, P. K.; Dar, R.A.; Tiwari, S.; Pitre, K. S. *Colloids Surf. A* **2012**, *396*, 8-15.
33. Atta, N. F.; El-Ads, E. H.; Galal, A. *J. Electrochem. Soc.* **2016**, *163*, B325-B334.

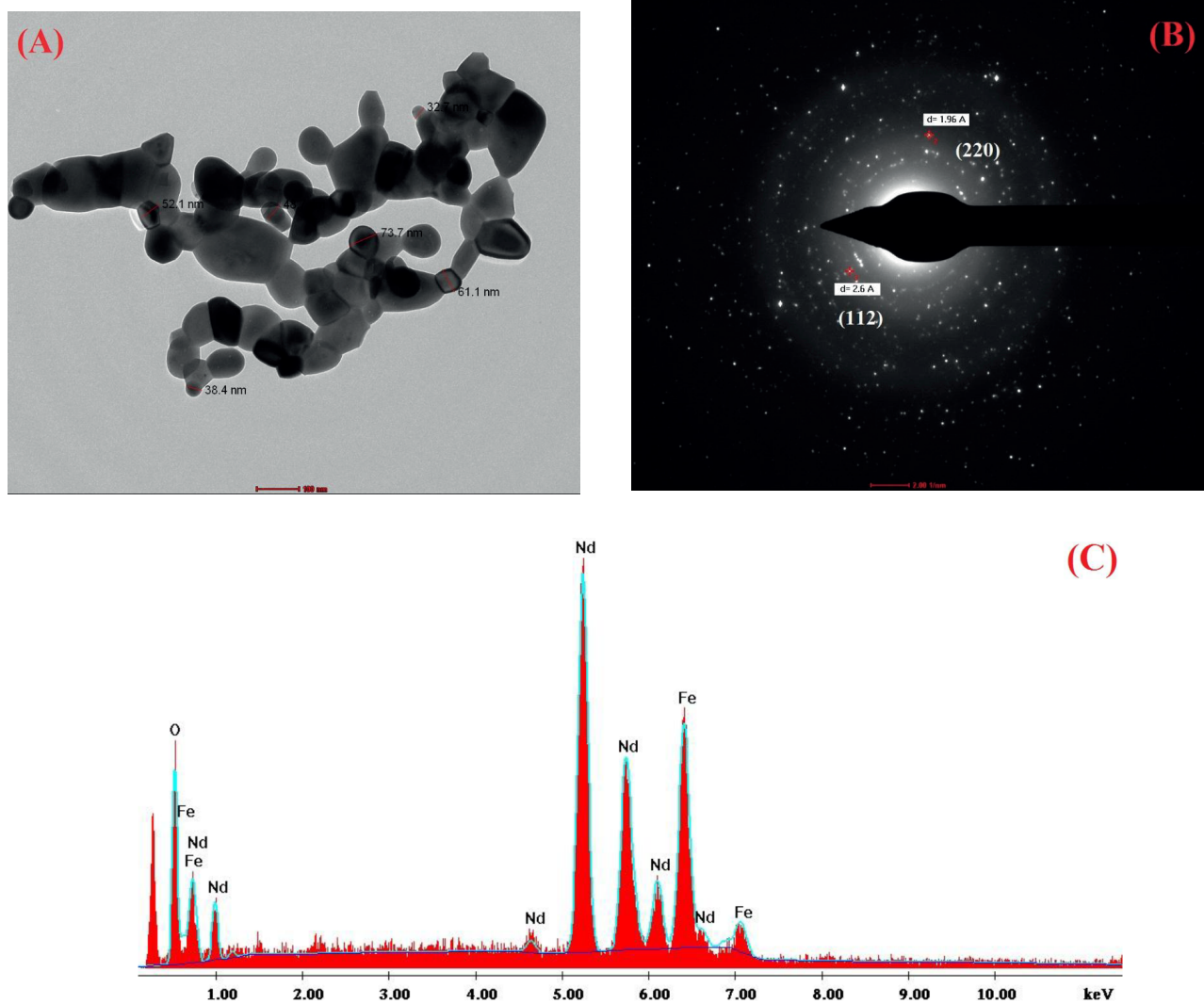
34. Navarro, M. C.; Pannunzio-Miner, E. V.; Pagola, S.; Gómez, M. I.; Carbonio, R. E. *J. Solid State Chem.* **2005**, *178*, 847-854.
35. Ghoreishi, M. S.; Behpour, M.; Zahrani, H. A.; Golestaneh, M. *Anal. Bioanal. Electrochem.* **2010**, *2*, 112- 124.
36. Al-Ghamdi, A. F.; Al-Ghamdi, A. H.; Al-Omar, M. A. *Egypt. J. Anal. Chem.* **2008**, *17*, 98-113.
37. Mokhtari, A.; Ghazaeian, M.; Maghsoudi, M.; Keyvanfard, M.; Emami, I. *Luminescence* **2015**, *30*, 1094-1100.
38. Mahmood, A. K. *Journal of Al-Nahrain University.* **2013**, *16*, 1-10.
39. Ryu, J.; Kim, K.; Kim, H.; Hahn, H.T.; Lashmore, D. *Biosens. Bioelectron.* **2010**, *26*, 602-607.

Supplementary Table. Structural parameters calculated from XRD data.

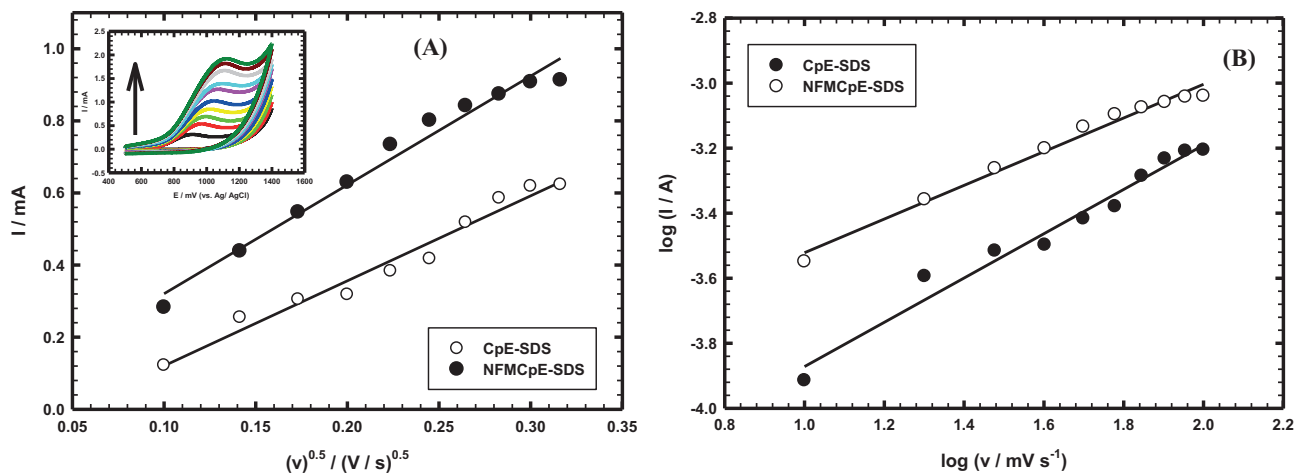
	Crystal structure	Lattice parameters, Å	Lattice volume, Å ³	Theoretical Density, g/cm ³	size, nm	factor
Standard NdFeO ₃ (card number 04-006-8303)	Orthorhombic	a = 5.4530 b = 5.5840 c = 7.7680	236.53	6.97	—	—
NdFeO ₃ citrate-nitrate method	Orthorhombic	a = 5.4326 b = 5.5834 c = 7.7886	236.25	6.97	36.80	0.9232



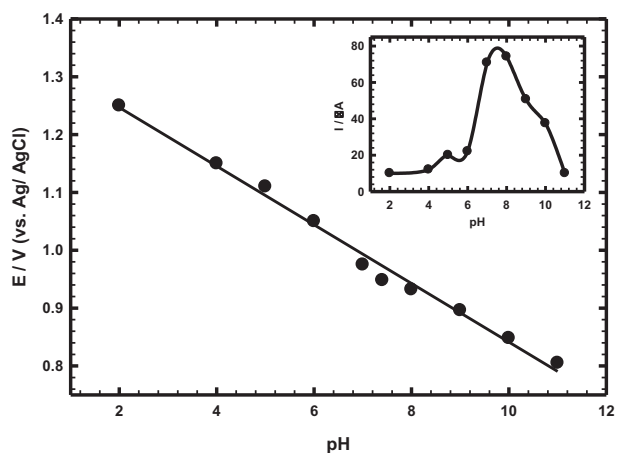
Supplementary Figure 1. A) XRD patterns of NdFeO₃ prepared by microwave assisted-citrate method. Miller indices (h, l, k) are given by black line. B) FTIR spectra of NdFeO₃ perovskite in the frequency range from 4000 to 400 cm⁻¹.



Supplementary Figure 2. A) TEM micrograph of NdFeO₃ perovskite; B) diffraction pattern obtained from the TEM measurement; C) EDAX measurement for NdFeO₃ perovskite.



Supplementary Figure 3. A) Plot of the anodic peak current values versus square root of scan rate for 0.5 mmol L^{-1} ketotifen/ 0.1 mol L^{-1} PBS/pH 7.40 at CpE-SDS (white circle) and NFMCPe-SDS (black circle). Inset: CVs of 0.5 mmol L^{-1} ketotifen/ 0.1 mol L^{-1} PBS/pH 7.40 at NFMCPe-SDS at different scan rates ($0.01\text{--}0.1 \text{ V s}^{-1}$). B) Plot of the logarithm of the anodic peak current values versus the logarithm of the scan rate for 0.5 mmol L^{-1} ketotifen/ 0.1 mol L^{-1} PBS/pH 7.40 at CpE-SDS (black circles) and NFMCPe-SDS (white circles).



Supplementary Figure 4. The relation between the anodic peak potential of 0.5 mmol L^{-1} ketotifen/ 0.1 mol L^{-1} PBS at NFMCPe-SDS and the pH values (2–11). Inset: relation between the anodic peak current of 0.5 mmol L^{-1} ketotifen/ 0.1 mol L^{-1} PBS at different pH values at NFMCPe-SDS.